Neurobiology of Pain 12 (2022) 100097

Contents lists available at ScienceDirect

Neurobiology of Pain

journal homepage: www.sciencedirect.com/journal/neurobiology-of-pain

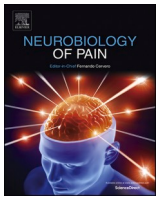

Original Research

Comprehensive phenotyping of cutaneous afferents reveals early-onset alterations in nociceptor response properties, release of CGRP, and hindpaw edema following spinal cord injury

Olivia C. Eller [a], Rena N. Stair [a], Christopher Neal [b], Peter S.N. Rowe [c,d], Jennifer Nelson-Brantley [a], Erin E. Young [a,e,f,g,h], Kyle M. Baumbauer [a,e,f,h,*]

[a] Department of Anatomy and Cell Biology, University of Kansas Medical Center, Kansas City, KS, United States
[b] Kansas Intellectual and Developmental Disabilities Research Center, University of Kansas Medical Center, Kansas City, KS, United States
[c] Department of Internal Medicine, University of Kansas Medical Center, Kansas City, KS, United States
[d] The Kidney Institute & Division of Nephrology, University of Kansas Medical Center, Kansas City, KS, United States
[e] Department of Anesthesiology, University of Kansas Medical Center, Kansas City, KS, United States
[f] Center for Advancement in Managing Pain, School of Nursing, University of Connecticut, Storrs, CT, United States
[g] Department of Genetics and Genome Sciences, UConn Health, Farmington, CT, United States
[h] Department of Neuroscience, UConn Health, Farmington, CT, United States

ARTICLE INFO

Keywords:
Acute spinal cord injury
Below level
Pain
DRG
Sensory neuron
Inflammation

ABSTRACT

Spinal cord injury (SCI) is a complex syndrome that has profound effects on patient well-being, including the development of medically-resistant chronic pain. The mechanisms underlying SCI pain have been the subject of thorough investigation but remain poorly understood. While the majority of the research has focused on changes occurring within and surrounding the site of injury in the spinal cord, there is now a consensus that alterations within the peripheral nervous system, namely sensitization of nociceptors, contribute to the development and maintenance of chronic SCI pain. Using an *ex vivo* skin/nerve/DRG/spinal cord preparation to characterize afferent response properties following SCI, we found that SCI increased mechanical and thermal responding, as well as the incidence of spontaneous activity (SA) and afterdischarge (AD), in below-level C-fiber nociceptors 24 hr following injury relative to naïve controls. Interestingly, the distribution of nociceptors that exhibit SA and AD are not identical, and the development of SA was observed more frequently in nociceptors with low heat thresholds, while AD was found more frequently in nociceptors with high heat thresholds. We also found that SCI resulted in hindpaw edema and elevated cutaneous calcitonin gene-related peptide (CGRP) concentration that were not observed in naïve mice. These results suggest that SCI causes a rapidly developing nociceptor sensitization and peripheral inflammation that may contribute to the early emergence and persistence of chronic SCI pain.

Introduction

Spinal cord injury (SCI) can have devastating consequences that are most commonly associated with loss of motor function. Individuals with SCI experience a number of additional complications, with the majority of patients experiencing chronic pain that is often severe (Brinkhof et al., 2016; Cruz-Almeida et al., 2005; Finnerup et al., 2001; Hulsebosch et al., 2009; McColl et al., 2012; Rekand et al., 2012; Richards, 2005; Siddall et al., 2003). This is significant because ongoing pain may impair recovery for those undergoing rehabilitation (Grau et al., 2004; Hook et al., 2008; Baumbauer and Grau, 2011; Baumbauer et al., 2008; Baumbauer et al., 2012). Unfortunately, current pain management relies on opioids, despite research demonstrating that these drugs are unsuccessful at treating chronic pain and can even exacerbate functional loss associated with injury (e.g., bowel motility), potentiate the development of pain, and undermine locomotor recovery (Aceves et al., 2019; Attal et al., 2010; Bryce, 2018; Frank et al., 2016; Hook et al., 2007; Woller and Hook, 2013). With the absence of viable alternatives to opioids

* Corresponding author at: Department of Anatomy and Cell Biology, University of Kansas Medical Center, 3901 Rainbow Blvd, MS 3051, Kansas City, KS 66160, United States.
E-mail address: kbaumbauer@kumc.edu (K.M. Baumbauer).

https://doi.org/10.1016/j.ynpai.2022.100097
Received 29 December 2021; Received in revised form 9 June 2022; Accepted 10 June 2022
Available online 17 June 2022

there is a need to better understand the mechanisms underlying SCI pain to improve treatment options and patient quality of life.

Pain following SCI is identified regionally by the relationship of pain experience to the site of injury. At-level pain is reported in dermatomes and myotomes that are innervated by sensory neurons originating from the injury site. Below-level pain, by comparison, originates from tissue below the level of injury (Hagen and Rekand, 2015; Soler et al., 2010), and is unique because it occurs despite disrupted connectivity in the ascending neural pathways and in the absence of normal somatosensation (Siddall and Loeser, 2001). This type of pain occurs in the majority of SCI pain patients (Burke et al., 2017), and is characterized as a spontaneous, intense burning or stabbing sensation that is refractory to current medical intervention (Burke et al., 2017).

While the mechanisms underlying below-level pain are complex, there is significant evidence demonstrating that nociceptors contribute to the development and maintenance of SCI-induced pain (Bavencoffe et al., 2016; Bedi et al., 2010; Carlton et al., 2009; Carlton et al., 2011; Yang et al., 2014). Furthermore, while the majority of SCI pain is not reported for weeks to months after injury, research suggests that increases in nociceptor excitability, such as the emergence of spontaneous activity (SA), may occur within days following SCI. Because SA is known to underly spontaneous pain (Bedi et al., 2010; Carlton et al., 2009; Devor, 2009; Djouhri et al., 2006; North et al., 2019; Odem et al., 2018; Ray et al., 2019; Wall and Devor, 1983; Yang et al., 2014), these findings suggest that the peripheral neuronal plasticity that contributes to the development of pathological pain are engaged well before patient pain reports. However, a knowledge gap exists in our understanding of the relationship between incidence of SA and other types of aberrant nociceptor activity, such as afterdischarge (AD), and whether SCI alters response properties in specific functional populations of nociceptors. Here we show that SCI increases responding to mechanical and thermal stimulation, as well as the incidence of SA and AD, in unmyelinated nociceptors. The incidence of SA and AD was significantly correlated with thermal, but not mechanical, sensitivity, with SA observed in low threshold heat responsive nociceptors and AD observed in high threshold heat responsive nociceptors. Interestingly, these alterations in nociceptor functional response properties were observed 24 hr following injury and were also associated with the development of hindpaw edema and increased cutaneous calcitonin gene related peptide (CGRP), suggesting that SCI produces peripheral inflammation during the acute phase of injury that may also contribute to continued nociceptor sensitization. This work is an important step in establishing the mechanisms underlying SCI pain by further supporting the role of the peripheral nervous system in the development of pathological pain following SCI.

Methods

Animals

Experiments were conducted using 8–12 week-old (20–30 g) female C57BL/6J mice (Jackson Laboratories, Bar Harbor, ME) that were group housed (4–5 mice/cage) and maintained in a temperature-controlled environment on a 12:12 light:dark cycle with free access to food and water. Female mice were used because women may be more likely to develop pain (Bartley and Fillingim, 2013; Greenspan et al., 2007; Sorge et al., 2011), research suggests that women may also be at greater risk of developing SCI pain (Dijkers et al., 2009; Norrbrink Budh et al., 2003; Werhagen et al., 2007), and because the mechanisms underlying the development of pain in biologic females is underrepresented. All studies were approved by the UConn Health and University of Kansas Medical Center Institutional Animal Care and Use Committee and treated in accordance with published NIH standards.

Spinal contusion injury

Mice were randomly assigned to SCI and naïve conditions and SCI mice were anesthetized with isoflurane (2%). SCI was produced by making a rostro-caudal incision along the vertebral midline to expose the thoracic level vertebrae and surrounding musculature. Tissue was carefully removed from around the vertebral column, and a laminectomy was performed at the level of T8-T11 using fine surgical scissors and forceps (Fine Science Tools; Foster City, CA). The spinal column was then secured into position on the impactor using modified forceps (Fine Science Tools; Foster City, CA) clamped to vertebral tissue rostral and caudal of T8 and T11, respectively. Dorsal spinal contusions were produced at the T9 spinal level using the Infinite Horizons IH-0400 Spinal Cord Impactor (Precision Systems and Instrumentation; Lexington, KY) equipped with a standard mouse impact tip (1.3 mm diameter) at a severity of 65 kDynes (kD) with a 1 s dwell time (range = 65–72 kD, average = 67 ± 0.40 kD). The T9 spinal level was chosen to leave the lumbar spinal cord and dorsal root projections intact. Following the contusion, the wound was closed with 7–0 vicryl sutures, mice were injected with 2 mL of 0.9% saline and 5 mg/kg of gentamicin sulfate and were placed on warm heating pads until regaining consciousness. Once regaining consciousness, mice were individually housed in cages with enrichment materials (plastic huts, burrowing material, etc.), and food, water, and supplemental gel diet (ClearH_2O, Westbrook, ME) were placed in specially designed containers on the cage floor. Cages were placed on warm heating pads such that half of the cage remained off the heating pad in quiet rooms away from foot traffic. Locomotor ability was assessed 24 hr following SCI, and only mice having scores ≤ 1 on the Basso Mouse Scale (BMS) were included in the study (Basso et al., 2006). Because SCI is a polytraumatic injury that can include damage to multiple tissues, including skin, muscle, and bone, that collectively influence pain development, and because prior work has shown that performing laminectomies alone in sham controls is sufficient to produce nociceptor sensitization and long-lasting pain in mice (Odem et al., 2018; Odem et al., 2019), we used naïve mice as controls to understand how pathophysiological nociceptor function produced by polytraumatic SCI compares to nociceptor function in the uninjured, naïve state. While useful for showing the effects of polytraumatic SCI, this experimental design does limit experimental inferences that can be made about the effects of SCI alone.

Micro computed tomography (μCT) and spinal cord contrast imaging.

SCI and naïve mice were anesthetized with a lethal exposure to isoflurane and intracardially perfused with ice cold 0.9% saline followed by 4% paraformaldehyde solution in phosphate buffered saline (PFAPBS). Whole spinal cords were carefully removed, post-fixed for 24 h in PFAPBS at 4 °C, and then suspended in a solution containing 260 mg/mL iohexol (Omnipaque™; GE Healthcare, Marlborough, MA) in 70% ethanol at 4 °C for 7 days. Spinal cords were then wrapped and heat-sealed in cling film to prevent dehydration and stacked in a μCT sample container (12 mm diameter × 75 mm height) for batch analysis. Samples were scanned using a Scanco μCT40 imaging system supported by a Hewlett Packard Integrity itanium Server rx2660 with dual core itanium processors 32 GB memory and Open VMS operating system (Scanco Medical USA, Inc – Southeastern, PA 19399). The cone-beam μCT40 system has a peak energy input range of 30 to 70kVp, a maximum scan/sample size 36.9 × 80 mm with a 6 μm resolution capability. A specific *batch control file* for spinal cord contrast analysis was used with the following specifications: **1.** Energy Intensity 45 kVp, 177 μA and 8 W; **2.** A FOV/Diameter of 12 mm with a voxel (VOX) resolution size of 6 μM; **3.** Integration time 300 mS and, **4.** Data Averaging = 7. Following raw data acquisition and computer reconstruction the 6 μM *.DCIM output files were contoured and defined using the "Scanco" software morph or integration functions. Further descriptions are provided in our previous publications (Curry et al., 2020; David et al., 2009; Lorensen and Cline, 1987; Rowe et al., 2006; Rowe et al., 2015; Staines et al., 2012; Zelenchuk et al., 2015; Zelenchuk et al., 2014; Zelenchuk et al., 2015). Other groups have also used μCT to assess injury

parameters and have found that μCT images are comparable to commonly used myelin staining and even provide more relevant information on spinal cord grey and white matter anatomical structures (Saito et al., 2012; Zambrano-Rodriguez et al., 2021). 3D Slicer (https://www.slicer.org) was used to process *.DCIM files for image reconstruction using the Segment Editor module.

Ex vivo preparation and electrophysiological recordings.

The *ex vivo* skin/nerve/DRG/spinal cord preparation (depicted in Fig. 1) is similar to what has been described elsewhere (Adelman et al., 2019; Baumbauer et al., 2015; Jankowski et al., 2017; Koerber and Woodbury, 2002; Lawson et al., 2008; McIlwrath et al., 2007; Molliver et al., 2016; Woodbury et al., 2001). Briefly, mice were anesthetized with an intraperitoneal (i.p.) injection of a 90/10 mg/kg mixture of ketamine and xylazine and were then transcardially perfused with ice cold oxygenated (95% O2–5% CO2) artificial cerebrospinal fluid (aCSF; in mM: 1.9 KCl, 1.2 KH2PO4, 1.3 MgSO4, 2.4 CaCl2, 26.0 NaHCO3, 10.0 D-glucose, and 127.0 NaCl). The spinal cord, saphenous nerve, DRG, and hindpaw skin were dissected in continuity and transferred to a recording chamber also containing oxygenated aCSF. The skin was placed on an elevated metal platform so that the epidermis was exposed to air and the subdermal layers remained in contact with 31 °C bath aCSF. This orientation of the skin allows for mechanical and thermal stimulation of the epidermal surface in a naturalistic manner while maintaining viability of the preparation.

Electrophysiological recordings were performed by impaling individual sensory neuron somata with sharp quartz microelectrodes containing 1 M potassium acetate. Orthograde electrical search stimuli were administered through a suction electrode placed on the saphenous nerve to locate sensory neuron somata innervating the skin. Receptive fields were localized on the skin using mechanical (e.g., paintbrush) or thermal stimuli (~51 °C or ~ 0 °C 0.9% saline). Response characteristics of DRG neurons were determined by applying digitally controlled mechanical and thermal stimuli. The mechanical stimulator consisted of a tension/length controller (Aurora Scientific, Aurora, ON, Canada) attached to a 1-mm diameter plastic disk. Computer controlled 5-s square waves of 1, 5, 10, 25, 50, and 100 mN were applied to each cell's receptive field. After mechanical stimulation, a controlled thermal stimulus was applied using a 2 × 3 mm contact area Peltier element (Yale University Machine Shop, New Haven, CT, USA). The temperature stimulus consisted of a 12 s heat ramp from 31 °C to 52 °C, followed by a 5-s holding phase, after which the temperature was ramped back down to 31 °C over a 12 s period. A 30 s resting period was inserted between stimulus presentations. In some instances, fibers could not be characterized by computer-controlled mechanical and/or thermal stimulation but were able to be phenotyped using von Frey and/or saline stimuli, respectively. These cells were not included in threshold determination. All elicited responses were recorded digitally for offline analysis (Spike 2 software, Cambridge Electronic Design, Cambridge, UK). Action potential firing that occurred in the absence of stimulation was defined as "spontaneous activity (SA)", while action potential firing that occurred following the termination of mechanical or thermal stimulation and that lasted for at least 1 s was defined as "afterdischarge (AD)".

Peripheral conduction velocity was then calculated from spike latency and the distance between stimulation and recording electrodes (measured directly along the saphenous nerve). Fibers with conduction velocities (CVs) $>$ 10 m/s were classified as conducting at Aβ velocity, fibers with CVs $<$ 10 m/s and $>$ 1.2 m/s were classified as conducting in the Aδ range, and fibers with CVs $<$ 1.2 m/s were classified as conducting a C velocity (Lawson et al., 1993; Lawson and Waddell, 1991). A-fibers were further classified as low or high threshold mechanoreceptors (A-LTMR and A-HTMR, respectively), with HTMRs responding to forces $\geq$ 10mN. C-fibers were classified as follows: (1) those that responded to mechanical and heat stimuli (CMH); (2) cells that responded to mechanical, heat and cold stimulation (CMHC); (3) those that responded only to mechanical stimulation of the skin (CM); (4) those that responded to mechanical and cooling stimuli (but not heating) (CMC); (5) those that were cold and mechanically insensitive, but heat sensitive (CH); and (6) those that were heat and mechanically insensitive but responded to cooling of the skin (CC).

Enzyme-linked immunosorbent assays (ELISA)

Mice were anesthetized with a lethal exposure to isoflurane and intracardially perfused with ice cold 0.9% saline prior to the dissection and collection of hindpaw skin.

Hindpaw hairy skin was homogenized in ice-cold RIPA buffer/protease inhibitor cocktail and centrifuged for 20 min (4 °C; 18,000 rcf). Each sample's total protein concentration was determined using Pierce

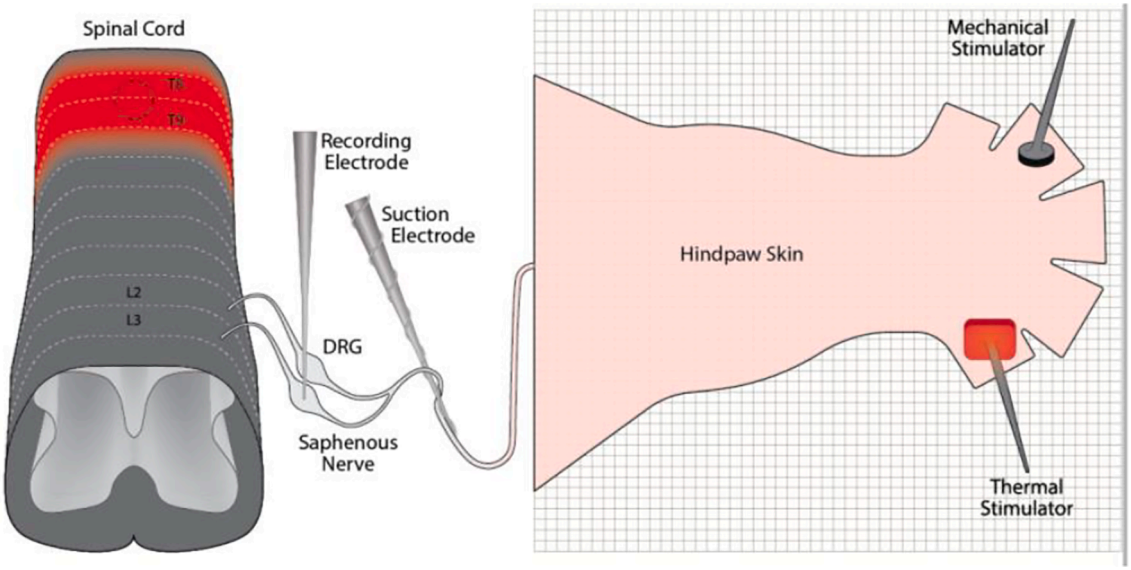

Fig. 1. Schematic depicting *ex vivo* skin/nerve/DRG/spinal cord preparation. Spinal contusion injury was performed at T8-T9, as shown in the red area. Spinal cord tissue rostral to the lesion site and caudal of L4 was dissected, leaving L2 and L3 DRG and the saphenous nerve in continuity with the hairy skin of the hindpaw. Sharp electrode recordings were performed by impaling neuron cell bodies contained within L2 and L3 DRG while heat, cold, and mechanical stimuli were delivered within the cutaneous receptive field of the neuron. (For interpretation of the references to color in this figure legend, the reader is referred to the web version of this article.)

BCA Protein Assay Kit (Thermo Fisher Scientific; Waltham, MA). ELISAs for CGRP (MyBioSource; San Diego, CA), substance P (SP; Enzo; Farmingdale, NY), and nerve growth factor β (NGFβ; Boster Bio; Pleasanton, CA) were run according to manufacturer's instructions. All samples were run in duplicate and absorbance ratios were read at 450 nm. Protein concentration was determined by comparison to linearized protein concentration standards, and analyses were conducted using the mean concentration for the duplicate wells for each sample.

Statistical analysis

Afferent population distribution data and the presence of SA and AD within specific functional populations of neurons were analyzed using a Fisher's exact test. Mean mechanical, heat, and cold thresholds, as well as mean resting membrane potentials (RMPs), were analyzed using Student's t-tests. Mechanical and heat firing rates were analyzed using mixed designs univariate analysis of variance (ANOVA) to account for treatment condition and mechanical force or temperature of stimulation, respectively, using Tukey's honestly significant difference (HSD) t-tests for *post hoc* testing where appropriate. Linear regression was used to determine relationships between SA and AD. Significance was determined using p values ≤ 0.05.

Results

Anatomic localization and characterization of spinal lesion

To confirm that potential alterations in below-level nociceptor function were not caused by direct damage to the L2-L3 segments of the spinal cord, the anatomic region where the saphenous nerve terminals project centrally, location and characterization of thoracic contusion injury was performed using μCT imaging (n = 3/condition). The total length of the spinal segment of interest was measured and the lesion epicenter was determined as the point an equal distance from both healthy margins (indicated as 0 mm), where the defining anatomic characteristics of the dorsal and ventral horns are absent. A total of 6

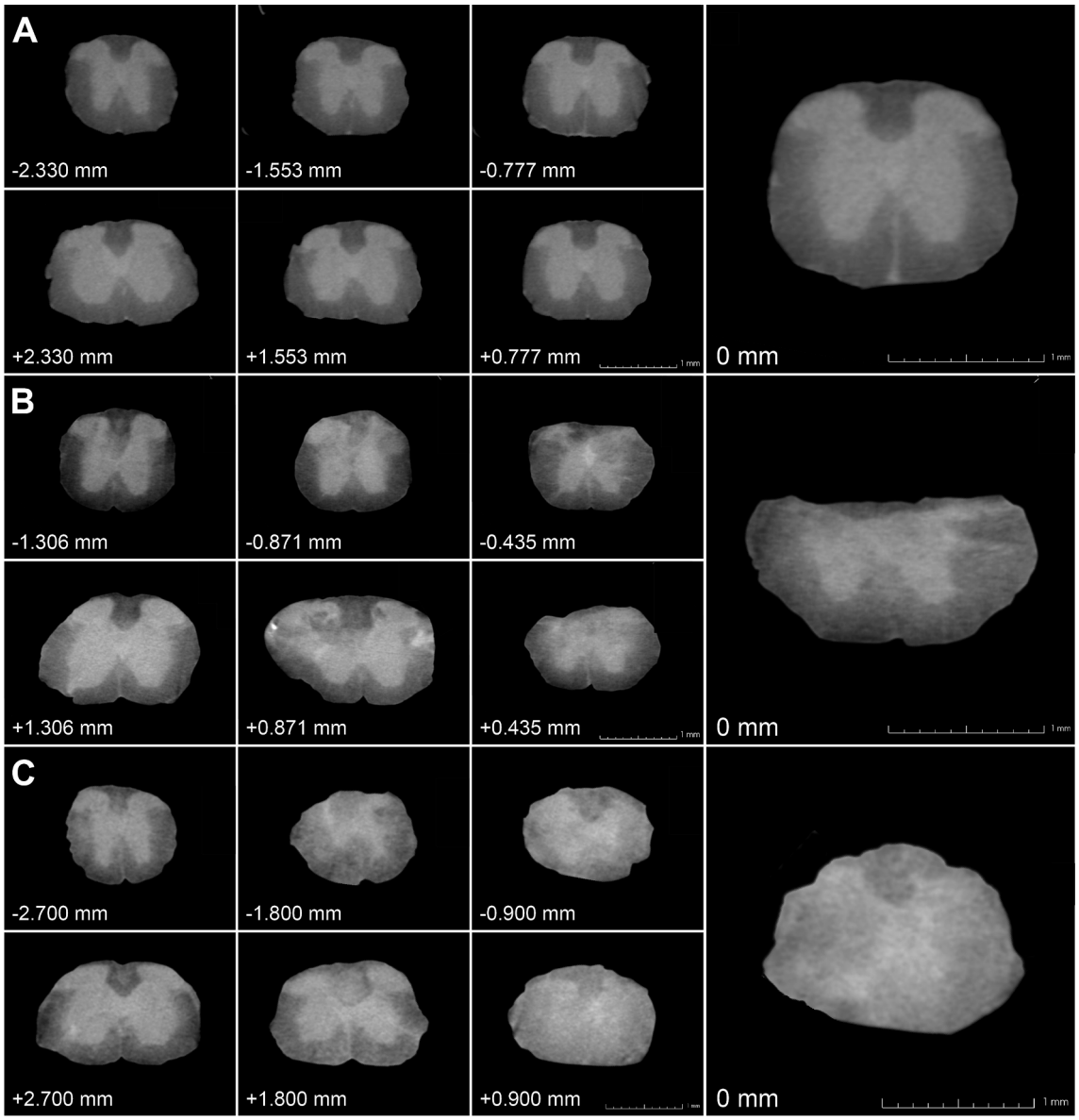

Fig. 2. μCT visualization of naïve (A), SCI 1 day (B), and SCI 7 day (C) spinal cords depicting rostral (- mm) and caudal (+mm) cross-sections taken at evenly distributed increments from the lesion epicenter (0 mm). The lesion epicenter and borders were determined by gross anatomic deformity on gray and white matter. Scale bars = 1 mm.

slices were then selected at evenly distributed increments rostrally and caudally from the epicenter to determine the extent of the lesion and confirm whether the contusion directly affected L2-L3 spinal segments and saphenous nerve dorsal roots. We found no evidence of damage to the saphenous nerve roots or L2-L3 white and gray matter (Fig. 2A–C).

Functionally identified afferent populations in naïve and SCI mice 24 hr following injury

We performed *ex vivo* intracellular sharp electrode electrophysiological recordings on 67 cutaneous primary afferents from 19 naïve mice and 81 cutaneous primary afferents from 27 SCI mice. All recordings were performed 24 hr following SCI. We first analyzed afferent response characteristics broadly based on responses to mechanical and temperature stimuli applied to the skin. Analyses revealed that 61.2% of naïve neurons (n = 41) responded to temperature, and of that population 58.2% responded to heat (n = 39) and 11.9% (n = 8) responded to cold (Table 1). We also found that 88.1% were mechanically sensitive (n = 59), with 46.3% responding to both mechanical and heat stimulation (n = 31), 11.9% responding to mechanical and cold stimulation (n = 8), and 9.0% responding to mechanical, heat, and cold stimulation (n = 6). Additional analyses demonstrated that 64.2% of SCI neurons were temperature sensitive (n = 52), with 56.8% responding to heat (n = 46) and 18.5% responding to cold (n = 15). Furthermore, 84.0% were sensitive to mechanical stimulation, with 44.4% being sensitive to mechanical and heat stimulation (n = 68), 14.8% responding to mechanical and cold stimulation (n = 12), and 11.1% (n = 9) were sensitive to mechanical, heat, and cold stimulation (Table 1). Statistical comparison of these distributions revealed a significantly greater proportion of SCI afferents that were sensitive to cold stimulation compared to the naïve, $\chi^2 = 4.08$, $p < .05$. No other significant relationships were found.

We further characterized neurons by fiber type (A vs C) and further divided nociceptors into subpopulations based on specific stimulus-evoked response using the methods described above to distinguish fiber types (see Table 2). The afferent phenotype distribution for naïve neurons included 16.4% A-LTMR (n = 11), 13.4% A-HTMR (n = 9), 9.0% CM (n = 6), 11.9% CH (n = 8), 0.0% CC, 3.0% CMC (n = 2), 37.3% CMH (n = 25), and 9.0% CMHC (n = 6) neurons. The distribution of SCI afferents included 12.4% A-LTMR (n = 10), 16.1% A-HTMR (n = 13), 7.4% CM (n = 6), 12.4% CH (n = 10), 3.7% CC (n = 3), 3.7% CMC (n = 3), 33.3% CMH (n = 27), and 11.1% CMHC (n = 9) neurons. Analysis of the distribution of cells between each group failed to reveal any significant differences in the proportion of neuronal subtypes represented in either naïve or SCI conditions (Table 2).

SCI increases mechanical sensitivity in unmyelinated C-fiber nociceptors 24 hr following injury

We assessed mechanical thresholds from 11 naïve and 10 SCI A-LTMR afferents 24 hr following SCI and found no difference in mean mechanical thresholds between naïve (4.27 ± 0.47 mN) and SCI (3.67 ± 0.63 mN) neurons (Fig. 3A). Similar results were also observed when comparing mechanical thresholds of 9 naïve (49.09 ± 17.34 mN) and 13 SCI (33.08 ± 6.58 mN) A-HTMR afferents (Fig. 3B). Additional analysis of A-LTMR and A-HTMR firing rates in response to mechanical stimulation of the skin at 1, 5, 10, 25, 50, and 100 mN of force revealed no significant differences in firing rates in SCI relative to naïve A-fibers (Fig. 3C, 3D).

Analysis of mean mechanical thresholds from 6 naïve (87.50 ± 11.41 mN) and 6 SCI (75.00 ± 27.54) CM, 25 naïve (37.60 ± 10.61 mN) and 27 SCI CMH (24.23 ± 5.04 mN), and 6 naïve (36.67 ± 12.78 mN) and 9 SCI CMHC (11.50 ± 5.29 mN) neurons failed to detect significant differences between conditions (Fig. 4A–C). Interestingly, increased mechanically-evoked firing rates were observed in SCI CM neurons in response to 5, 10, 25, and 50 mN of force applied to the skin, SCI CMH neurons in response to 5 and 50 mN of force, and SCI CMHC neurons in response to 1 and 5 mN of force, all Fs > 4.86, $p < .05$ (Fig. 4D–F). We were able to characterize firing properties of 2 naïve and 3 SCI CMC neurons (data not shown) but did not perform statistical analysis due to the low sample size. Collectively, the above results suggest that SCI increases mechanical responding in C-fiber nociceptors within 24 hr of injury.

SCI increases thermal responsiveness in C-fiber nociceptors 24 hr following injury.

Temperature thresholds were also examined 24 hr following SCI from 8 naïve and 15 SCI cold sensitive neurons, 4 naïve and 10 SCI neurons that responded to warming of the skin, and 42 naïve and 46 SCI heat sensitive neurons. Analysis failed to reveal and significant differences in heat, cold, or warming response thresholds (Fig. 5**A–C**), as well as any significant differences in cold-evoked firing rates. No significant relationship was detected in the number of neurons that responded to warming of the skin between conditions. Analysis of heat-evoked firing rates showed that SCI CMH and CMHC nociceptors exhibited significantly increased firing rates in response to temperatures ranging from 31 to 38 °C and 41–51 °C, all Fs > 4.37, $p < .05$. Additional analysis found that SCI resulted in a significant increase in firing rate in CH nociceptors following 33–35 °C and 49–50 °C relative to naïve CH nociceptors, all Fs > 5.29, $p < .05$ (Fig. 6A–C), collectively demonstrating that SCI increases responsiveness in heat sensitive nociceptors.

SCI increases spontaneous activity and afterdischarge in C-fiber nociceptors 24 hr following injury.

Previous research has shown that SCI increases the incidence of SA and AD in putative nociceptors within days of injury and that SA and AD can persist for several months (Bavencoffe et al., 2016; Bedi et al., 2010; Pitcher and Henry, 2000; Woolf and McMahon, 1985; Yang et al., 2014). The prevalence of AD in nociceptors following SCI has not been well characterized, and it is not known whether SA and AD are interrelated, whether SA and AD are characteristics of a certain functional population of afferents, or whether an association exists between SCI-induced alterations in thermal and mechanical response thresholds and the incidence of SA or AD. To examine these issues, we first assessed the presence of SA in all electrophysiologically characterized neurons and found statistically greater proportion of SCI neurons (32/81) that exhibited SA relative to naïve neurons (1/67), Fisher's exact test, $p < .0001$. When we analyzed the presence of SA in specific functional subtypes of afferents, we found that 0/11 naïve and 2/10 SCI LTMRs, 0/9 naïve and 0/13 SCI HTMRs, 1/6 naïve and 5/6 SCI CMs, 0/8 naïve and 6/10 SCI CHs, 0/2 naïve and 1/3 SCI CMCs, 0/25 naïve and 14/27 SCI CMHs, and 0/6 naïve and 4/9 SCI CMHCs exhibited SA. Analysis of these data revealed a significant increase in the occurrence of SA in SCI relative to naïve CMH neurons, Fisher's exact test, $p < .00001$. (Fig. 7**A**). We next examined the prevalence of AD in SCI nociceptor and found that

Table 1
Distribution (%) of naïve and SCI afferents that respond to temperature, mechanical, and the combination of temperature and mechanical, stimuli. The percentage of afferents within each category did not differ between conditions except for the percentage of cold responding afferents from SCI mice (bold). *=significantly different from naïve, Fisher's exact test, $p < .05$.

Stimulus Modality	Naïve % responders	SCI % responders
Temperature	61.2	64.2
Heat	58.2	56.8
Cold	11.9	**18.5***
Mechanical	88.1	84.0
Mechanical + Heat	46.3	44.4
Mechanical + Cold	11.9	14.8
Mecahnical + Heat + Cold	9.0	11.1

Table 2
Functional population distributions of characterized primary afferent populations from naïve (A) and SCI (B) mice 24 hr following injury. Both groups of mice show similar distributions of A- and C-fibers as well as resting membrane potentials (RMP). However, analysis did reveal an increase in the percentage of CC neurons characterized from SCI mice, *=statistical significance relative to naïve mice, Fisher's exact test, *t*-test, $p < .05$.

Phenotype	Fiber Type	Function	% Naïve (N = 67)	%SCI (N = 81)	Naïve RMP (mV)	SCI RMP (mV)
A-LTMR	A	Low threshold mechanoreceptor	16.4	12.4	−46.61 ± 3.63	−56.13 ± 4.20
A-HTMR	A	High threshold mechanoreceptor	13.4	16.1	−53.45 ± 4.28	−60.12 ± 3.69
CM	C	Mechanoreceptor	9.0	7.4	−42.13 ± 6.36	−50.30 ± 3.41
CC	C	Cold sensitive	0.0	3.7	–	−39.43 ± 5.43
CH	C	Heat sensitive	11.9	12.4	−39.65 ± 4.25	−44.69 ± 4.69
CMC	C	Mechanical + cold sensitive	3.0	3.7	−42.25 ± 0.67	−58.50 ± 5.93
CMH	C	Mechanical + heat sensitive	37.3	33.3	−46.13 ± 1.93	−44.23 ± 2.02
CMHC	C	Mechanical + heat + cold sensitive	9.0	11.1	−53.07 ± 3.56	−49.40 ± 2.47

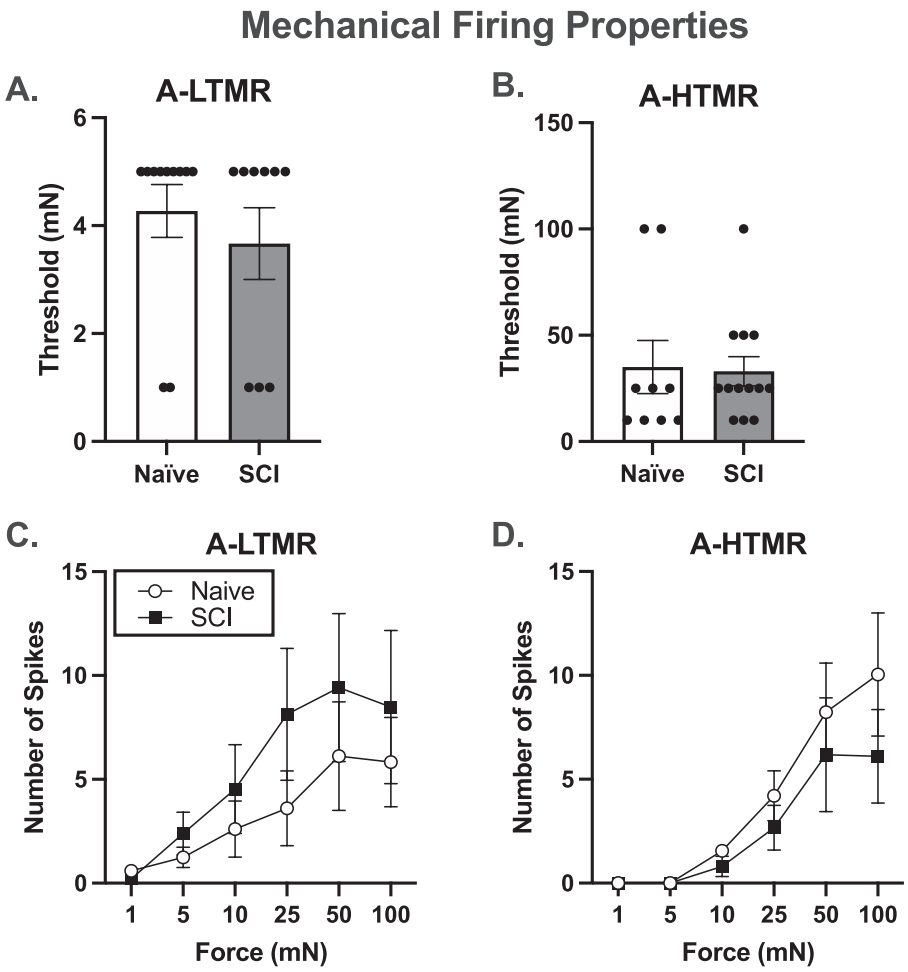

Fig. 3. Analysis of mechanically evoked response thresholds and force-dependent firing rates from naïve (n = 11) and SCI (n = 10) A-LTMRs (A, C) and naïve (n = 9) and SCI (n = 13) A-HTMRs (B, D) 24 hr following SCI. No significant differences in mean threshold or firing rates emerged, *t*-test, ANOVA, all $p > .05$.

while AD was absent in all naïve neurons, we did observe AD in 34/81 of SCI neurons, Fisher's exact test, $p < .0001$. Quantification of the presence of AD within in each functional subclass of SCI neurons showed that 1/10 LTMRs, 0/13 HTMRs, 4/6 CMs, 0/10 CHs, 1/3 CMCs, 23/27 CMHs, and 5/9 CMHCs exhibited AD (Fig. 7B). This relationship was driven by a statistically significant increase in AD occurrence in SCI relative to naïve CMH and CMHC nociceptors, all Fisher's exact tests, $p < .05$. Representative traces illustrating our collective findings can be seen in Fig. 8A–F.

It is possible that the increase in SA and AD following SCI was due to alterations in the intrinsic electrophysiological properties of neurons, potentially resulting in a relative state of depolarization and a subsequent decrease in firing threshold. To examine this possibility, we compared resting membrane potentials (RMPs) in each neuronal subtype across injury conditions. We found no significant differences in RMPs in any subpopulation of afferents following SCI compared to naïve subjects (Table 2).

SA and AD occur in similar functional distributions of nociceptive afferents in response to SCI. Pearson correlations were then performed to determine whether there was an association between the presence of SA and AD in a given cell and failed to detect any significant relationships ($r_P = 0.048$, $p > .05$). We then examined whether nociceptor phenotype, mechanical sensitivity, or heat sensitivity was significantly correlated with SA or AD using linear regression. We failed to resolve

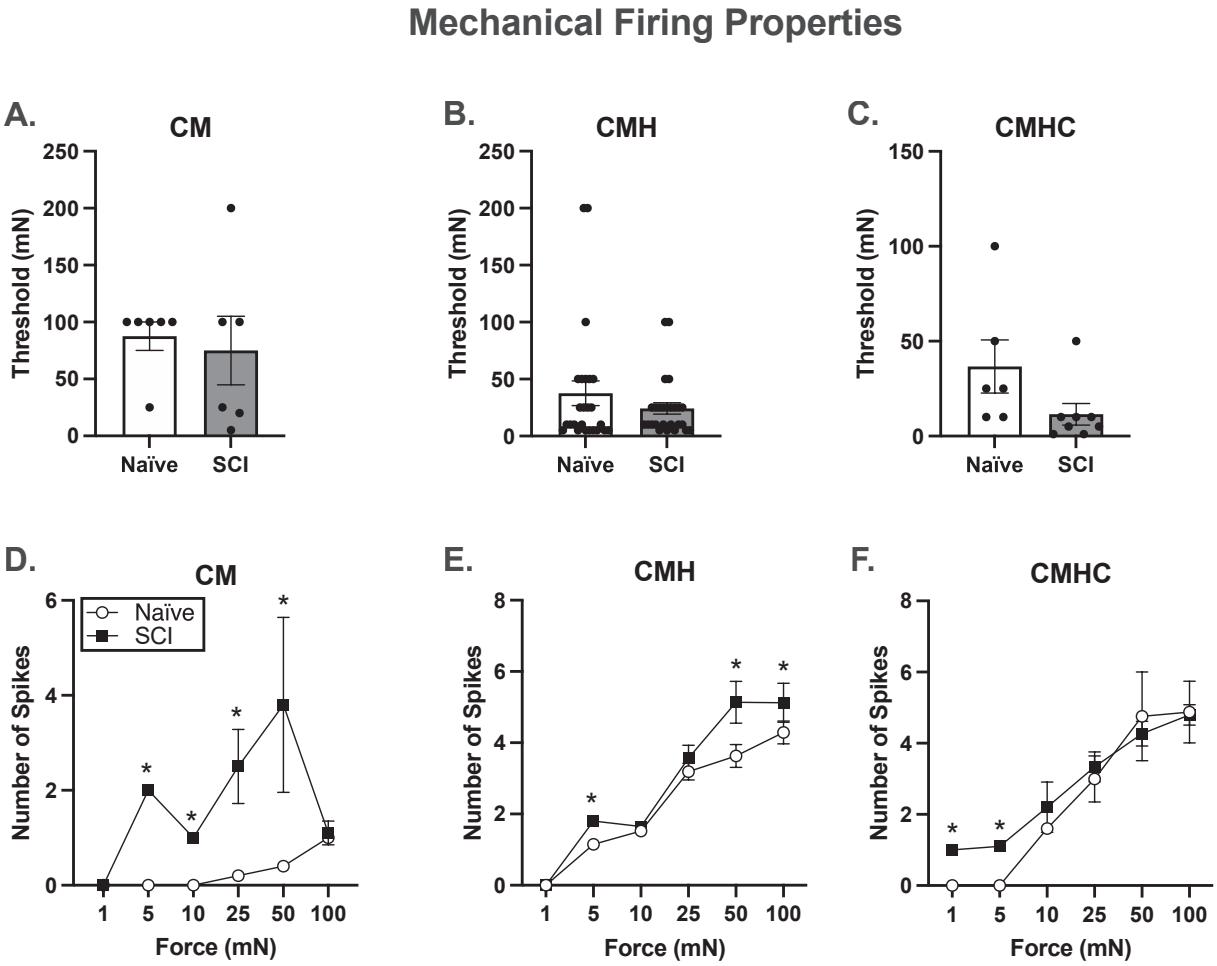

Fig. 4. C-fiber mechanical response thresholds and force-dependent firing rates. Response thresholds and firing rates are shown for naïve (n = 6) and SCI (n = 6) CM (A, D), naïve (n = 25) and SCI (n = 27) CMH (B, E), and naïve (n = 6) and SCI (n = 9) CMHC (C, F) nociceptors 24 hr following SCI. While mean mechanical thresholds were not statistically different between naïve and SCI conditions (*t*-test, $p > .05$), we observed a general increase in firing rates as greater force was applied to the skin. We also observed significantly increased firing rates in the lower range of stimulation in SCI relative to naïve neurons. *=significantly different from naïve, ANOVA, $p < .05$.

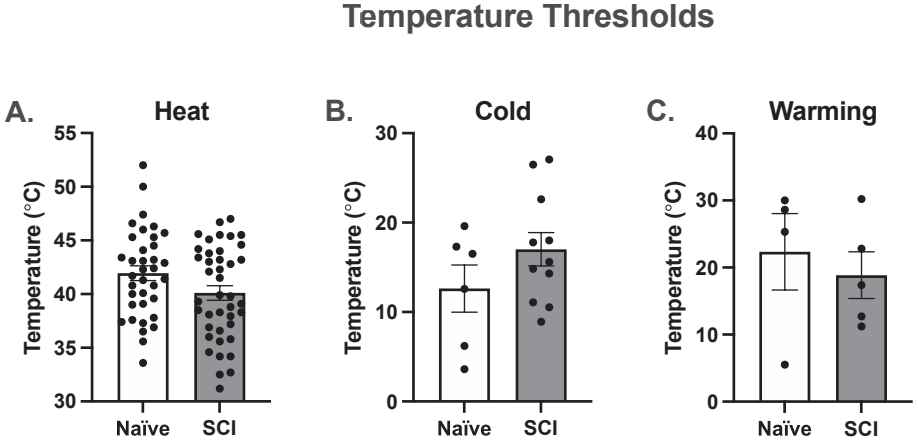

Fig. 5. C-fiber temperature response thresholds. Mean temperature-dependent response thresholds of naïve (n = 36) and SCI (n = 41) heat-sensitive (A) and naïve (n = 6) and SCI (n = 9) cold-sensitive nociceptors (B). Mean firing threshold for naïve (n = 4) and SCI (n = 5) nociceptors that fired AP in response to warming of the skin following cooling (C). No stimulus-specific differences were observed, *t*-test, all $p > .05$.

any significant association between specific nociceptor subtype or mechanical sensitivity with the incidence of SA or AD (all $r_P < 0.32$, $p < .05$). However, our analysis did reveal a significant inverse relationship between heat threshold and the presence of SA ($r_P = -0.290$, $p < .05$), as well as a significant positive relationship between heat threshold and the presence of AD ($r_P = 0.300$, $p < .05$). Collectively,

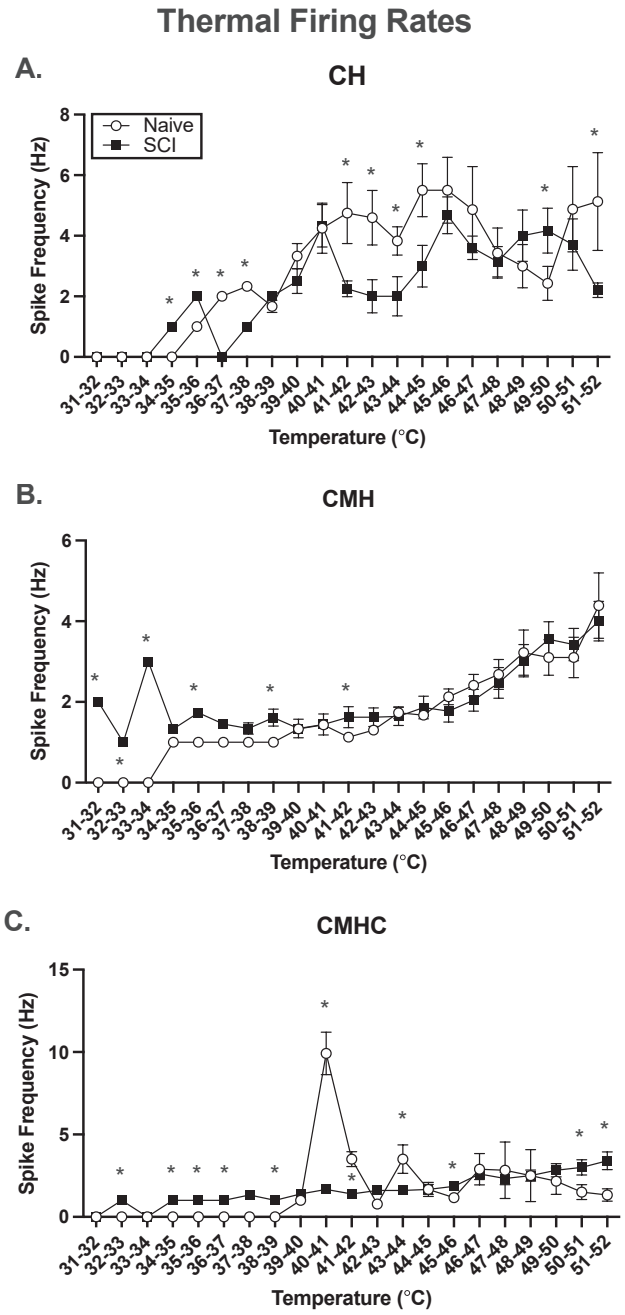

Fig. 6. Firing rates for thermally-sensitive nociceptors in response to increasing temperature. Firing rates are depicted for naïve (n = 8) and SCI (n = 10) CH (A), naïve (n = 25) and SCI (n = 27) CMH (B), and naïve (n = 6) and SCI (n = 9) CMHC (C) nociceptors in response to a 12 s thermal ramp ranging from 31 to 52 °C. In general, we found that SCI increased thermal sensitivity, and SCI neurons fired in response to lower stimulation than naïve nociceptors. *=significantly different from naïve, ANOVA, all $p < .01$.

these results suggest that a population of low threshold heat-responsive nociceptors is more likely to exhibit SA, while a separate population of high threshold heat-responsive nociceptors is more likely to exhibit AD.

SCI increases hindpaw edema and cutaneous CGRP occurrence of spontaneous pain behaviors in injured mice

Inflammation is a significant driver of both central and peripheral pain states (Chapman and Vierck, 2017; Gold and Gebhart, 2010; Ma et al., 2006; Price et al., 2018; Tal, 1999; Treede et al., 1992) and is often observed in the form of edema. To determine whether hindpaw edema was associated with inflammatory processes that developed during the acute phase of SCI, we measured paw thickness in a separate cohort of 10 naïve and 15 SCI mice during the first 7 days of recovery following SCI. We found that hindpaw diameter increased significantly following SCI relative to naïve mice. Latency (days) to reach peak hindpaw thickness did not differ between mice, however mean paw thickness was significantly greater in SCI (2.20 ± 0.09 mm) relative to naïve (1.85 ± 0.09 mm) mice, $t(24) = 2.71$, $p < .05$ (Fig. 9A).

Hindpaw edema results from increased release of proinflammatory molecules within the microenvironment of the skin, including CGRP, NGF, and SP (Amann et al., 1996; Dansereau et al., 2021; Garry and Hargreaves, 1992; Queiroz et al., 2018; Siney and Brain, 1996). Concentration of each of these respective proteins was measured in hindpaw skin lysate 24 hr following SCI. Our analysis did not detect any change in NGF or SP concentrations following SCI. However, CGRP levels in hindpaw skin were significantly elevated following SCI, $t(24) = 2.10$, $p < .05$ (Fig. 9B–D), suggesting the presence of acute-onset CGRP-dependent inflammation within the skin.

Discussion

SCI increases spontaneous pain behavior, neurogenic-like inflammation, and nociceptor sensitivity

Chronic pain occurs at an alarmingly greater percentage in the spinally injured relative to the general chronic pain population (Cruz-Almeida et al., 2005; Finnerup et al., 2001; Hulsebosch et al., 2009; Rekand et al., 2012; Siddall et al., 2003), is often poorly managed, and is associated with poor prognoses for recovery (Grau et al., 2004; Hook et al., 2008; Baumbauer and Grau, 2011; Baumbauer et al., 2008; Baumbauer et al., 2012). The mechanisms underlying SCI-induced pain are initiated rapidly following injury (Bedi et al., 2010), and our present results demonstrate that hindpaw edema, and increased CGRP levels occurred 1–7 days following injury, suggesting that injured animals experience ongoing pain via a neurogenic inflammation-like process that could augment nociceptor response properties.

Given the above results we next examined potential SCI-induced alterations in nociceptor response properties during the first 24 hr following SCI. The majority of characterized neurons from both naïve and SCI mice were mechanically sensitive, with a smaller, but significant, proportion of afferents that were temperature sensitive. The distribution of temperature-responsive neurons was similar between conditions, with the exception of increased cold-sensitive afferents after SCI. However, this finding should be interpreted with some caution because we did not characterize any CC neurons from naïve mice, which is unusual.

Alterations in afferent response characteristics appear to emerge due to increased sensitivity within specific functional populations of neurons. We did not observe changes in mechanical response thresholds or firing rates in A-fiber afferents. We did observe increased action potential (AP) firing in response to mechanical force applied to the skin that was independent of changes in mean mechanical response thresholds in C-fiber afferents, with CM, CMH and CMHC nociceptors exhibiting a leftward shift in mechanical sensitivity; CM nociceptors exhibited increased firing in response to 5–50 mN of force, CMH nociceptors exhibited increased firing in response to 5 and 50 mN of force, and CMHC nociceptors exhibited increased firing in response to 1 and 5 mN of force applied to the skin. Importantly, while CM and CMH nociceptors increased their firing in response to noxious levels of stimulation (>5 mN), all of the characterized nociceptors exhibited increased firing rates to stimulation at or near innocuous forces, suggesting that normally innocuous mechanical stimulation may heighten nociceptor responding that potentially contributes to increased pain (e.g., allodynia) after SCI. Furthermore, given that SCI also increased AP firing in response to 10–50 mN of applied force in CM nociceptors and 50 mN of applied force

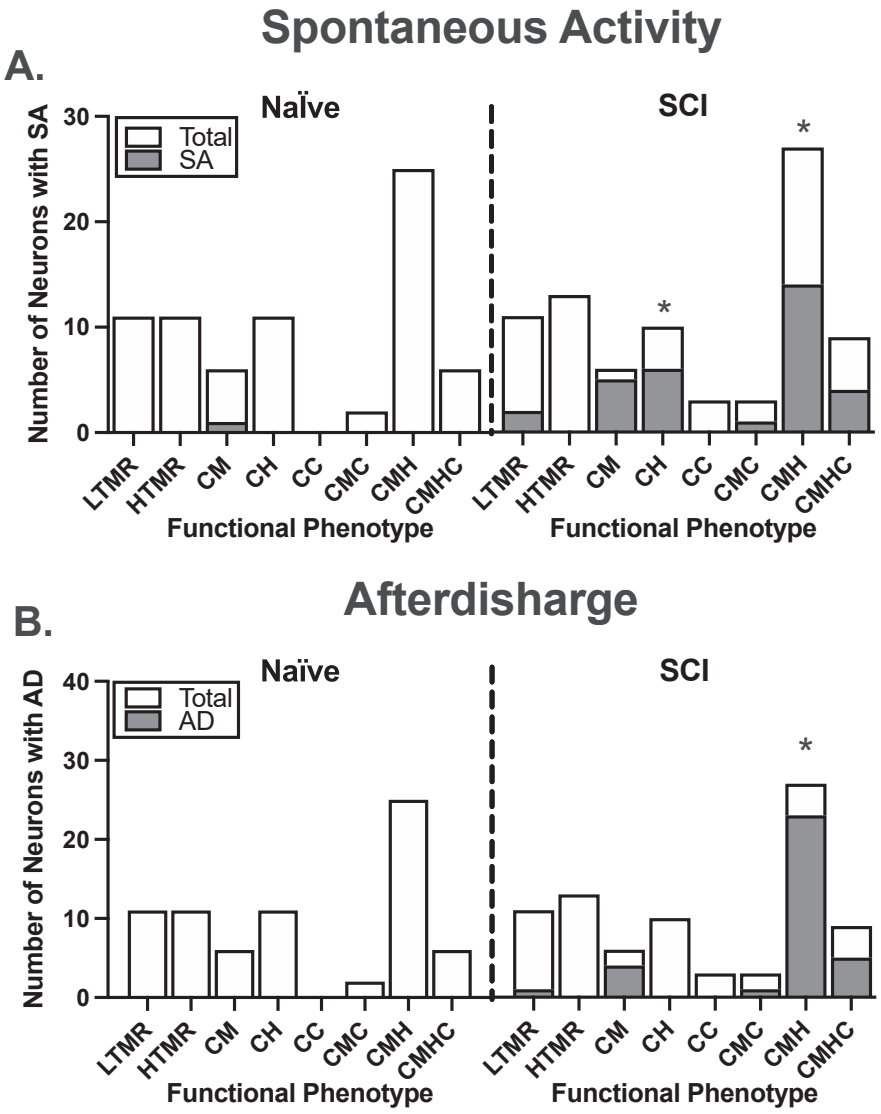

Fig. 7. Spontaneous activity (SA) and afterdischarge (AD) in functional subtypes of afferents. A) incidence of SA in characterized naïve and SCI afferents. Data are depicted as number of neurons that exhibited SA (gray bars) relative to total of characterized neurons (white bars). B) incidence of AD in characterized naïve and SCI neurons depicted as number of neurons that exhibited AD (gray bars) relative to total of characterized neurons (white bars). * = significant difference from naïve, Fisher's exact test, $p < .05$.

in CMH nociceptors, these results suggest that activation of these specific subpopulations of nociceptors by noxious mechanical stimulation increases activity that may promote development of hyperalgesia.

Application of hot, warm, and cold stimuli to the skin did not reveal any significant differences in mean response thresholds or the number of nociceptors that responded to warming of the skin between naïve and SCI mice. However, we did find that thermally sensitive nociceptor populations (e.g., CH, CMH, and CMHC) exhibited leftward shifts in their respective temperature response curves following SCI; SCI CH nociceptors exhibited an increase in firing rate at 34 °C, while naïve CHs began firing at 35 °C; SCI CMH nociceptors began firing at 31 °C, while naïve CMHs began firing at 34 °C; and SCI CMHC nociceptors showed modest, but statistically significant, increases in firing at 32 °C, while naïve CMHCs began firing at 39 °C. Interestingly, we observed an increase in naïve CMHC firing between 39 °C and 42 °C that was not observed in SCI CMHC nociceptors. We have observed this same firing function in the past, and it appears to be altered as a result of genetic overexpression of neurturin (Jankowski et al., 2017), knockdown of *P2ry1* (Jankowski et al., 2012), or deletion of *MrgprD* (Rau et al., 2009) or *P2ry2* (McIlwrath et al., 2007). Given that the SCI CMHC nociceptors show flat, consistent increases in firing across most temperatures without sharp increases in firing in specific temperature ranges, it is possible that SCI causes acute disruptions in neurotrophic factor or purinergic signaling that alter nociceptor function. In general, it can be concluded that exposure to increasing temperatures produced complex stimulation-response curves that could result from system-wide adaptations in response to injury, including spinal shock or energy deficiencies related to increased demands during the healing process and SCI-induced mitochondrial dysfunction (Sullivan et al., 2007).

SCI increases spontaneous activity and afterdischarge in specific populations of C-fiber nociceptors

SA has been observed in dissociated afferent cell bodies within 3 days of SCI, persists for at least 8 months following injury, and, importantly, leads to the development of chronic SCI pain (Bavencoffe et al., 2016; Bedi et al., 2010; Yang et al., 2014). These findings have been instrumental in establishing a role for peripheral neurons in the development and maintenance of chronic SCI pain. Here, we build upon this previous work by showing that SA develops in CH and CMH nociceptors, while AD emerges in CMH nociceptors, within 24 hr of SCI, which may suggest that other populations of neurons begin to show functional gains in spontaneous firing at differential rates following SCI. These results are important because they show that SA and AD develop acutely following SCI and that there are certain afferent populations that are more vulnerable to the effects of SCI. While SA and AD are found in similar

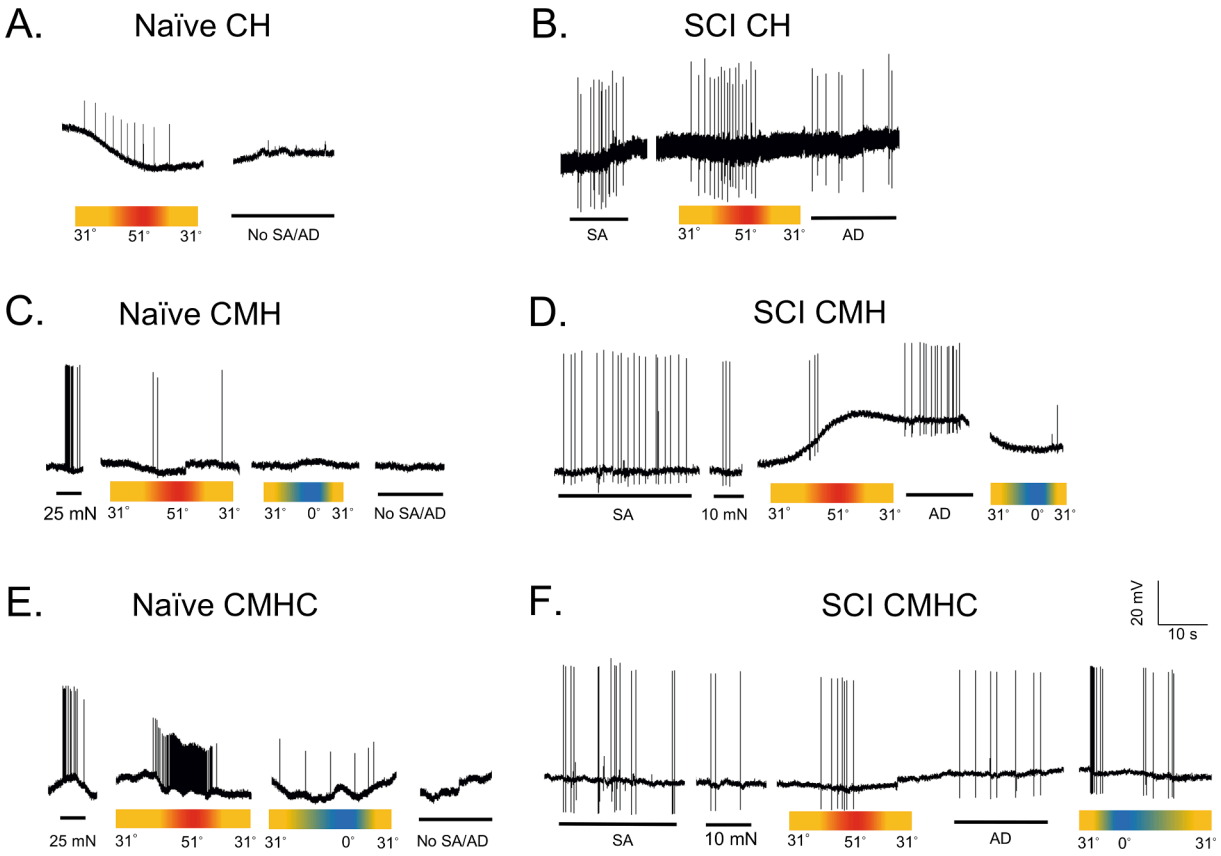

Fig. 8. Representative electrophysiological traces from naïve and SCI CH, CMH, and CMHC nociceptors. SCI CH nociceptors exhibit increased firing rates in response to innocuous and noxious heat stimuli relative to naive CH nociceptors (A, B). Naïve CMH and CMHC nociceptors respond to 25 mN of force (but not 10 mN; data not shown), while SCI CMH and CMHC nociceptors respond to 10 mN of force applied to the skin. SCI nociceptors also show SA and AD that is absent in naïve nociceptors (C-F). SCI increased the incidence of SA and AD across most functional populations of nociceptors, which was rarely observed in naïve neurons. Color coded bars represent heating and cooling ramp temperatures and rate of temperature change, and the scale bar indicates voltage (25 mV) and time (10 s).

functional populations of neurons, their relative distributions are not identical. The overall presence of SA and AD are not correlated with one another, suggesting that independent molecular processes may be responsible for their development, even within the same cell. In addition, we found independent relationships between SA, AD, and thermal, but not mechanical, sensitivity, where SA was correlated with lower heat thresholds while the presence of AD was correlated with higher heat thresholds. Interestingly, nociceptors that exhibited SA tended to have heat activation thresholds below 40 °C, while those that exhibited AD tended to have heat activation thresholds above 40 °C, suggesting that different populations of heat transducers may contribute to the emergence of SA and AD. For example, channels with temperature sensitivity below 40 °C, such as P2X3 and TRPV3 (Grandl et al., 2008; Hoffstaetter et al., 2018; Khmyz et al., 2008; Moqrich et al., 2005; Smith et al., 2002; Xu et al., 2002), may be responsible for the development of SA in low heat threshold nociceptors, while channels whose temperature sensitivity is>40 °C, such as TRPM3, TRPV1, and TRPV2 (Caterina et al., 1999; Hoffstaetter et al., 2018; Liu and Qin, 2016; Vriens et al., 2011), may contribute to AD. How specific channels may contribute to SCI-induced SA and AD is not currently known, but it is possible that SCI causes injury-dependent increases in channel sensitivity or functional coupling of channels such as TRPA1 and TRPV1 or TRPM3 and TRPV1, that may alter nociceptor firing properties. Finally, it is also possible that SA and AD are not governed by different cellular mechanisms and that the transduction of various stimuli by select channels may result in transient periods of "aftersuppression" that pause ongoing SA. Once aftersuppression has subsided, SA may then re-emerge, giving the appearance of the development of AD. If SA and AD are mechanistically similar, and presentation of specific stimuli causes aftersuppression, then there may be molecules common to SA and AD that can be targeted for therapeutic intervention, and that may also be able to be disrupted by presentation of environmental stimuli.

While further work is needed to detail the above mechanisms, our results indicate that low threshold nociceptors may fire continuously in the presence and absence of stimulation, while high threshold nociceptors may continue to fire despite termination of a heat stimulus, both of which may initiate miscoding of sensory input. Moreover, because below-level nociceptors exhibit increases in excitability, it is also possible that SCI causes widespread thermal and mechanical sensitivity between systems (e.g., musculoskeletal, cutaneous, visceral) that may lead to indiscriminable widespread pain (Walters, 2012). It is important to note that one limitation of our experiments is that we did not include a sham control condition and used naïve mice as controls. Therefore, it is possible that the alterations in nociceptor function observed may have been due to tissue damage resulting from the surgical procedure (e.g., damage to muscle, bone, etc.) and not solely injury to the spinal cord itself (Odem et al., 2018; Odem et al., 2019). Nonetheless, our data also suggest that the polytraumatic nature of SCI, including injury to nervous and surrounding tissues, alters functional properties of uninjured nociceptors located below the anatomic level of the injury.

Central-to-peripheral signaling may recruit and maintain firing of below-level nociceptors via neurogenic inflammation

The emergence of SA and AD in specific populations of C-fiber nociceptors within the first 24 hr following SCI further underscores how central injury affects peripheral nociceptor function, even when the tissue innervated by those nociceptors is undamaged. This dysfunctional

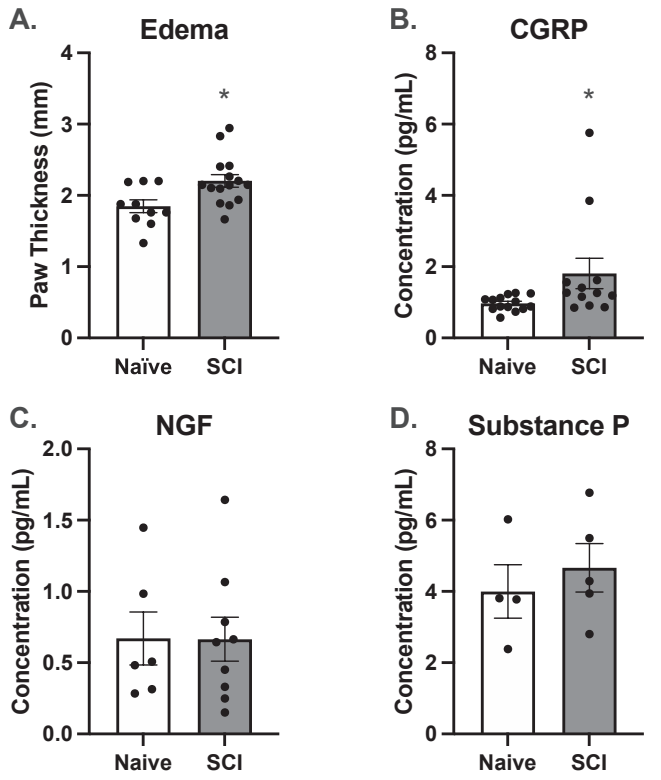

Fig. 9. Analysis of hindpaw edema and concentrations of cutaneous CGRP, NGF, and SP. Edema (A) was determined by increased paw thickness (mm) in SCI (n = 15) relative to naïve (n = 10) mice. (B) Mean concentrations of CGRP in naïve (n = 14) and SCI (n = 12) hindpaw skin 24 hr following injury. (C) Mean concentrations of NGF found in naïve (n = 6) and SCI (n = 9) hindpaw skin 24 hr following injury. (D) Mean concentrations of SP found in naïve (n = 4) and SCI (n = 5) SP hindpaw skin 24 hr following injury. We found that SCI increased paw thickness and concentration of CGRP present in the skin. * = significant difference from naïve, *t*-test, $p < .05$.

nociceptor plasticity might emerge through a centrally driven mechanism within the spinal cord that activates receptors or channels expressed on the central terminals of below-level nociceptors, ultimately resulting in the generation of antidromic nociceptor AP generation. Prior work has shown that SCI increases the early release of proinflammatory cytokines, such as IL-1β, in the spinal cord that increase afferent sensitivity (Obreja et al., 2002), while *in vitro* experiments examining DRG neuron excitability has shown that that IL-1β may produce increased excitability by altering voltage-gated Na + channel conductance (Noh et al., 2019). Consequently, it is possible that increased proinflammatory cytokine release could result in the generation of spontaneous antidromic action potentials that travel toward the periphery, causing the release of neuropeptides, including CGRP, from the peripheral terminals of nociceptors, resulting in vasodilation and edema that is independent of a classic immune response, a process known as neurogenic inflammation (Chiu et al., 2012; Hou et al., 2003; Levine et al., 1985). Prostaglandins, ATP, cytokines, and nerve growth factor (NGF) are also released by immune cells during this process, and binding to their cognate receptors expressed directly on nociceptors can further potentiate AP firing (Brain and Williams, 1985; Cruwys et al., 1992; Kessler et al., 1999; Roza and Reeh, 2001). However, in the case of SCI, this process can occur in the absence of peripheral tissue damage, without an obvious need for a host defense or wound healing response, and the presence of neuroactive molecules involved in neurogenic inflammation, such as CGRP, may activate peripheral nociceptor terminals, initiating or maintaining further SA, AD, and alterations in stimulus evoked nociceptor responding. Moreover, given that central and peripheral inflammatory stimulation may persistently drive ectopic afferent activity following SCI, this constant nociceptor activation may further increase stimulus sensitivity and excitability, similar to what has been observed following induction of wind-up, central sensitization, and long-term potentiation (Cook et al., 1987; Ji et al., 2003; Ji and Woolf, 2001; Ma and Woolf, 1995; Sivilotti et al., 1993; Sun et al., 2004; Wall and Woolf, 1984; Wall and Woolf, 1986; Woolf, 1996; Xu et al., 1992; Xu et al., 1995; Sandkuhler et al., 2006; Sandkuhler, 2007; Sandkuhler and Liu, 1998). While previous work has shown that the development of SA results from depolarizing RMPs, reductions in AP threshold, and the occurrence of depolarizing spontaneous fluctuations (DSFs) (Odem et al., 2018), we were unable to replicate those findings. This discrepancy may have resulted from differences in electrophysiological techniques used in each study and the inherent limitations associated with sharp electrode recordings, such as recording instability and decreased input resistance, that make accurate measurement of RMPs and detection of DSFs less reliable than what can be obtained during whole cell patch clamp recordings, for example.

Functional and clinical importance of altered evoked and spontaneous nociceptor firing properties

Activation of nociceptors following SCI may create a "reverberatory loop", where antidromic nociceptor APs generated in the injured spinal cord causes release of neuroactive molecules from peripheral terminals (e.g., CGRP) into their targets of innervation (Walters, 2012), causing generation and propagation of orthodromic nociceptor APs into the spinal cord that fosters the development and/or maintenance of an excitatory environment within the spinal cord. Consequently, breaking this self-perpetuating loop of nociceptive communication could serve as a valuable mechanistic target for treating chronic SCI pain by silencing nociceptor output. Furthermore, treatments that disrupt nociceptor output could be administered during the first few hours following SCI, when nociceptor output is increasing, with the intent of preventing pain development. In laboratory settings this approach has been highly successful and experimental work has repeatedly shown that prevention of chronic pain development is possible while reversal of chronic pain is incredibly difficult. Therefore, prophylactic intervention close to the time of injury may be successful in preventing the later onset of chronic SCI pain.

Activation of nociceptors by innocuous mechanical or thermal stimuli suggests that numerous endogenous or environmental stimuli have the potential to cause pain and could have detrimental effects for patient pain burden and recovery. These stimuli could include normal body temperature, limb movement, mechanical forces involved in gastrointestinal function, contact with wheelchairs, bedsheets, clothing, and administration of necessary medical procedures (e.g., catheterization, IV placement, etc.). Consequently, therapeutics designed to quiet nociceptor activity during the acute phase of injury may have broad reaching effects by improving patient recovery prognosis and quality of life.

CRediT authorship contribution statement

Olivia C. Eller: Conceptualization, Methodology, Validation, Formal analysis, Investigation, Supervision, Funding acquisition. **Rena N. Stair:** Validation, Formal analysis, Investigation, Funding acquisition. **Christopher Neal:** Conceptualization, Formal analysis, Visualization. **Peter S.N. Rowe:** Conceptualization, Formal analysis, Investigation, Visualization. **Jennifer Nelson-Brantley:** Investigation, Supervision, Project administration. **Erin E. Young:** Conceptualization, Methodology, Formal analysis, Resources, Supervision. **Kyle M. Baumbauer:** Conceptualization, Methodology, Validation, Formal analysis, Investigation, Resources, Supervision, Funding acquisition.

Declaration of Competing Interest

The authors declare that they have no known competing financial

interests or personal relationships that could have appeared to influence the work reported in this paper.

Acknowledgments

This work was supported by NIH grants R03 NS096454 (KMB), R21 NS104789 (KMB), the Rita Allen Foundation Award in Pain (KMB), the KUMC Biomedical Research Training Program (OCE), the Madison and Lila Self Graduate Fellowship (RNS), the Kansas Institutional Development Award (IDeA) P20 GM103418, and core support from the Kansas IDDRC P30 HD 000228.

Appendix A. Supplementary data

Supplementary data to this article can be found online at https://doi.org/10.1016/j.ynpai.2022.100097.

References

Aceves, M., Terminel, M.N., Okoreeh, A., Aceves, A.R., Gong, Y.M., Polanco, A., Sohrabji, F., Hook, M.A., 2019. Morphine increases macrophages at the lesion site following spinal cord injury: protective effects of minocycline. Brain Behav. Immun. 79, 125–138.

Adelman, P.C., Baumbauer, K.M., Friedman, R., Shah, M., Wright, M., Young, E., Jankowski, M.P., Albers, K.M., Koerber, H.R., 2019. Single-cell q-PCR derived expression profiles of identified sensory neurons. Mol. Pain 15, 1744806919884496.

Amann, R., Schuligoi, R., Herzeg, G., Donnerer, J., 1996. Intraplantar injection of nerve growth factor into the rat hind paw: local edema and effects on thermal nociceptive threshold. Pain 64 (2), 323–329.

Attal, N., Cruccu, G., Baron, R., Haanpaa, M., Hansson, P., Jensen, T.S., Nurmikko, T., 2010. European Federation of Neurological S. EFNS guidelines on the pharmacological treatment of neuropathic pain: 2010 revision. Eur. J. Neurol. 17 (9), 1113–e1188.

Bartley, E.J., Fillingim, R.B., 2013. Sex differences in pain: a brief review of clinical and experimental findings. Br. J. Anaesth. 111 (1), 52–58.

Basso, D.M., Fisher, L.C., Anderson, A.J., Jakeman, L.B., McTigue, D.M., Popovich, P.G., 2006. Basso mouse scale for locomotion detects differences in recovery after spinal cord injury in five common mouse strains. J. Neurotrauma 23 (5), 635–659.

Baumbauer KM, DeBerry JJ, Adelman PC, Miller RH, Hachisuka J, Lee KH, Ross SE, Koerber HR, Davis BM, Albers KM. Keratinocytes can modulate and directly initiate nociceptive responses. eLife 2015;4.

Baumbauer, K.M., Grau, J.W., 2011. Timing in the absence of supraspinal input III: regularly spaced cutaneous stimulation prevents and reverses the spinal learning deficit produced by peripheral inflammation. Behav. Neurosci. 125 (1), 37–45.

Baumbauer, K.M., Hoy Jr., K.C., Huie, J.R., Hughes, A.J., Woller, S.A., Puga, D.A., Setlow, B., Grau, J.W., 2008. Timing in the absence of supraspinal input I: variable, but not fixed, spaced stimulation of the sciatic nerve undermines spinally-mediated instrumental learning. Neuroscience 155 (4), 1030–1047.

Baumbauer, K.M., Lee, K.H., Puga, D.A., Woller, S.A., Hughes, A.J., Grau, J.W., 2012. Temporal regularity determines the impact of electrical stimulation on tactile reactivity and response to capsaicin in spinally transected rats. Neuroscience 227, 119–133.

Bavencoffe, A., Li, Y., Wu, Z., Yang, Q., Herrera, J., Kennedy, E.J., Walters, E.T., Dessauer, C.W., 2016. Persistent electrical activity in primary nociceptors after spinal cord injury is maintained by scaffolded adenylyl cyclase and protein kinase a and is associated with altered adenylyl cyclase regulation. J. Neurosci. 36 (5), 1660–1668.

Bedi, S.S., Yang, Q., Crook, R.J., Du, J., Wu, Z., Fishman, H.M., Grill, R.J., Carlton, S.M., Walters, E.T., 2010. Chronic spontaneous activity generated in the somata of primary nociceptors is associated with pain-related behavior after spinal cord injury. J. Neurosci. 30 (44), 14870–14882.

Brain, S.D., Williams, T.J., 1985. Inflammatory oedema induced by synergism between calcitonin gene-related peptide (CGRP) and mediators of increased vascular permeability. Br. J. Pharmacol. 86 (4), 855–860.

Brinkhof, M.W., Al-Khodairy, A., Eriks-Hoogland, I., Fekete, C., Hinrichs, T., Hund-Georgiadis, M., Meier, S., Scheel-Sailer, A., Schubert, M., Reinhardt, J.D., Swi, S.C.I. S.G., 2016. Health conditions in people with spinal cord injury: contemporary evidence from a population-based community survey in Switzerland. J. Rehabil. Med. 48 (2), 197–209.

Bryce, T.N., 2018. Opioids should not be prescribed for chronic pain after spinal cord injury. Spinal Cord Ser Cases 4, 66.

Burke, D., Fullen, B.M., Stokes, D., Lennon, O., 2017. Neuropathic pain prevalence following spinal cord injury: a systematic review and meta-analysis. Eur. J. Pain 21 (1), 29–44.

Carlton, S.M., Du, J., Tan, H.Y., Nesic, O., Hargett, G.L., Bopp, A.C., Yamani, A., Lin, Q., Willis, W.D., Hulsebosch, C.E., 2009. Peripheral and central sensitization in remote spinal cord regions contribute to central neuropathic pain after spinal cord injury. Pain 147 (1–3), 265–276.

Carlton, S.M., Du, J., Ding, Z., Yang, Q., Wu, Z., Walters, E.T., 2011. Hemisection of thoracic spinal cord results in chronic hyperexcitability in primary nociceptors that is expressed both in vivo and after dissociation. Society for Neuroscience Meeting Planner.

Caterina, M.J., Rosen, T.A., Tominaga, M., Brake, A.J., Julius, D., 1999. A capsaicin-receptor homologue with a high threshold for noxious heat. Nature 398 (6726), 436–441.

Chapman, C.R., Vierck, C.J., 2017. The transition of acute postoperative pain to chronic pain: an integrative overview of research on mechanisms. J. Pain 18 (4), 359. e1–359.e38.

Chiu, I.M., von Hehn, C.A., Woolf, C.J., 2012. Neurogenic inflammation and the peripheral nervous system in host defense and immunopathology. Nat. Neurosci. 15 (8), 1063–1067.

Cook, A.J., Woolf, C.J., Wall, P.D., McMahon, S.B., 1987. Dynamic receptive field plasticity in rat spinal cord dorsal horn following C-primary afferent input. Nature 325 (7000), 151–153.

Cruwys, S.C., Kidd, B.L., Mapp, P.I., Walsh, D.A., Blake, D.R., 1992. The effects of calcitonin gene-related peptide on formation of intra-articular oedema by inflammatory mediators. Br. J. Pharmacol. 107 (1), 116–119.

Cruz-Almeida, Y., Martinez-Arizala, A., Widerstrom-Noga, E.G., 2005. Chronicity of pain associated with spinal cord injury: a longitudinal analysis. J. Rehabil. Res. Dev. 42 (5), 585–594.

Curry, J.N., Saurette, M., Askari, M., Pei, L., Filla, M.B., Beggs, M.R., Rowe, P.S., Fields, T., Sommer, A.J., Tanikawa, C., Kamatani, Y., Evan, A.P., Totonchi, M., Alexander, R.T., Matsuda, K., Yu, A.S., 2020. Claudin-2 deficiency associates with hypercalciuria in mice and human kidney stone disease. J. Clin. Investig. 130 (4), 1948–1960.

Dansereau, M.A., Midavaine, E., Begin-Lavallee, V., Belkouch, M., Beaudet, N., Longpre, J.M., Melik-Parsadaniantz, S., Sarret, P., 2021. Mechanistic insights into the role of the chemokine CCL2/CCR2 axis in dorsal root ganglia to peripheral inflammation and pain hypersensitivity. J. Neuroinflamm. 18 (1), 79.

David, V., Martin, A., Hedge, A.M., Rowe, P.S., 2009. Matrix extracellular phosphoglycoprotein (MEPE) is a new bone renal hormone and vascularization modulator. Endocrinology 150 (9), 4012–4023.

Devor, M., 2009. Ectopic discharge in Abeta afferents as a source of neuropathic pain. Exp. Brain Res. 196 (1), 115–128.

Dijkers, M., Bryce, T., Zanca, J., 2009. Prevalence of chronic pain after traumatic spinal cord injury: a systematic review. J. Rehabil. Res. Dev. 46 (1), 13–29.

Djouhri, L., Koutsikou, S., Fang, X., McMullan, S., Lawson, S.N., 2006. Spontaneous pain, both neuropathic and inflammatory, is related to frequency of spontaneous firing in intact C-fiber nociceptors. J. Neurosci. 26 (4), 1281–1292.

Finnerup, N.B., Johannesen, I.L., Sindrup, S.H., Bach, F.W., Jensen, T.S., 2001. Pain and dysesthesia in patients with spinal cord injury: a postal survey. Spinal Cord 39 (5), 256–262.

Frank, J.W., Levy, C., Matlock, D.D., Calcaterra, S.L., Mueller, S.R., Koester, S., Binswanger, I.A., 2016. Patients' perspectives on tapering of chronic opioid therapy: a qualitative study. Pain Med. 17 (10), 1838–1847.

Garry, M.G., Hargreaves, K.M., 1992. Enhanced release of immunoreactive CGRP and substance P from spinal dorsal horn slices occurs during carrageenan inflammation. Brain Res. 582 (1), 139–142.

Gold, M.S., Gebhart, G.F., 2010. Nociceptor sensitization in pain pathogenesis. Nat. Med. 16 (11), 1248–1257.

Grandl, J., Hu, H., Bandell, M., Bursulaya, B., Schmidt, M., Petrus, M., Patapoutian, A., 2008. Pore region of TRPV3 ion channel is specifically required for heat activation. Nat. Neurosci. 11 (9), 1007–1013.

Grau, J.W., Washburn, S.N., Hook, M.A., Ferguson, A.R., Crown, E.D., Garcia, G., Bolding, K.A., Miranda, R.C., 2004. Uncontrollable stimulation undermines recovery after spinal cord injury. J. Neurotrauma 21 (12), 1795–1817.

Greenspan, J.D., Craft, R.M., LeResche, L., Arendt-Nielsen, L., Berkley, K.J., Fillingim, R. B., Gold, M.S., Holdcroft, A., Lautenbacher, S., Mayer, E.A., Mogil, J.S., Murphy, A. Z., Traub, R.J., 2007. Consensus working group of the Sex G, pain SIGotI. Studying sex and gender differences in pain and analgesia: a consensus report. Pain 132 (Suppl 1), S26–S45.

Hagen, E.M., Rekand, T., 2015. Management of neuropathic pain associated with spinal cord injury. Pain Ther. 4 (1), 51–65.

Hoffstaetter, L.J., Bagriantsev, S.N., Gracheva, E.O., 2018. TRPs et al.: a molecular toolkit for thermosensory adaptations. Pflugers Arch. 470 (5), 745–759.

Hook, M.A., Liu, G.T., Washburn, S.N., Ferguson, A.R., Bopp, A.C., Huie, J.R., Grau, J.W., 2007. The impact of morphine after a spinal cord injury. Behav. Brain Res. 179 (2), 281–293.

Hook, M.A., Huie, J.R., Grau, J.W., 2008. Peripheral inflammation undermines the plasticity of the isolated spinal cord. Behav. Neurosci. 122 (1), 233–249.

Hou, L., Li, W., Wang, X., 2003. Mechanism of interleukin-1 beta-induced calcitonin gene-related peptide production from dorsal root ganglion neurons of neonatal rats. J. Neurosci. Res. 73 (2), 188–197.

Hulsebosch, C.E., Hains, B.C., Crown, E.D., Carlton, S.M., 2009. Mechanisms of chronic central neuropathic pain after spinal cord injury. Brain Res. Rev. 60 (1), 202–213.

Jankowski, M.P., Rau, K.K., Soneji, D.J., Ekmann, K.M., Anderson, C.E., Molliver, D.C., Koerber, H.R., 2012. Purinergic receptor P2Y1 regulates polymodal C-fiber thermal thresholds and sensory neuron phenotypic switching during peripheral inflammation. Pain 153 (2), 410–419.

Jankowski, M.P., Baumbauer, K.M., Wang, T., Albers, K.M., Davis, B.M., Koerber, H.R., 2017. Cutaneous neurturin overexpression alters mechanical, thermal, and cold responsiveness in physiologically identified primary afferents. J. Neurophysiol. 117 (3), 1258–1265.

Ji, R.-R., Kohno, T., Moore, K.A., Woolf, C.J., 2003. Central sensitization and LTP: do pain and memory share similar mechanisms? Trends Neurosci. 26 (12), 696–705.

Ji, R.R., Woolf, C.J., 2001. Neuronal plasticity and signal transduction in nociceptive neurons: implications for the initiation and maintenance of pathological pain. Neurobiol. Dis. 8 (1), 1–10.
Kessler, F., Habelt, C., Averbeck, B., Reeh, P.W., Kress, M., 1999. Heat-induced release of CGRP from isolated rat skin and effects of bradykinin and the protein kinase C activator PMA. Pain 83 (2), 289–295.
Khmyz, V., Maximyuk, O., Teslenko, V., Verkhratsky, A., Krishtal, O., 2008. P2X3 receptor gating near normal body temperature. Pflugers Arch. 456 (2), 339–347.
Koerber, H.R., Woodbury, C.J., 2002. Comprehensive phenotyping of sensory neurons using an ex vivo somatosensory system. Physiol. Behav. 77 (4–5), 589–594.
Lawson, J.J., McIlwrath, S.L., Woodbury, C.J., Davis, B.M., Koerber, H.R., 2008. TRPV1 unlike TRPV2 is restricted to a subset of mechanically insensitive cutaneous nociceptors responding to heat. J. Pain 9 (4), 298–308.
Lawson, S.N., Waddell, P.J., 1991. Soma neurofilament immunoreactivity is related to cell size and fibre conduction velocity in rat primary sensory neurons. J. Physiol. 435, 41–63.
Lawson, S.N., Perry, M.J., Prabhakar, E., McCarthy, P.W., 1993. Primary sensory neurones: neurofilament, neuropeptides, and conduction velocity. Brain Res. Bull. 30 (3–4), 239–243.
Levine, J.D., Dardick, S.J., Basbaum, A.I., Scipio, E., 1985. Reflex neurogenic inflammation. I. Contribution of the peripheral nervous system to spatially remote inflammatory responses that follow injury. J. Neurosci. 5 (5), 1380–1386.
Liu, B., Qin, F., 2016. Use Dependence of Heat Sensitivity of Vanilloid Receptor TRPV2. Biophys. J . 110 (7), 1523–1537.
Lorensen, W.E., Cline, H.E., 1987. Marching cubes: A high resolution 3D surface construction algorithm. Comput Graphics 21 (4), 163–169.
Ma, C., Greenquist, K.W., Lamotte, R.H., 2006. Inflammatory mediators enhance the excitability of chronically compressed dorsal root ganglion neurons. J. Neurophysiol. 95 (4), 2098–2107.
Ma, Q.P., Woolf, C.J., 1995. Involvement of neurokinin receptors in the induction but not the maintenance of mechanical allodynia in rat flexor motoneurones. J. Physiol. 486 (Pt 3), 769–777.
McColl MA, Aiken A, McColl A, Sakakibara B, Smith K. Primary care of people with spinal cord injury: scoping review. Can Fam Physician 2012;58(11):1207-1216, e1626-1235.
McIlwrath, S.L., Lawson, J.J., Anderson, C.E., Albers, K.M., Koerber, H.R., 2007. Overexpression of neurotrophin-3 enhances the mechanical response properties of slowly adapting type 1 afferents and myelinated nociceptors. Eur. J. Neurosci. 26 (7), 1801–1812.
Molliver, D.C., Rau, K.K., Jankowski, M.P., Soneji, D.J., Baumbauer, K.M., Koerber, H.R., 2016. Deletion of the murine ATP/UTP receptor P2Y2 alters mechanical and thermal response properties in polymodal cutaneous afferents. Neuroscience 332, 223–230.
Moqrich, A., Hwang, S.W., Earley, T.J., Petrus, M.J., Murray, A.N., Spencer, K.S., Andahazy, M., Story, G.M., Patapoutian, A., 2005. Impaired thermosensation in mice lacking TRPV3, a heat and camphor sensor in the skin. Science 307 (5714), 1468–1472.
Noh, M.C., Stemkowski, P.L., Smith, P.A., 2019. Long-term actions of interleukin-1beta on K(+), Na(+) and Ca(2+) channel currents in small, IB4-positive dorsal root ganglion neurons; possible relevance to the etiology of neuropathic pain. J. Neuroimmunol. 332, 198–211.
Norrbrink Budh, C., Lund, I., Hultling, C., Levi, R., Werhagen, L., Ertzgaard, P., Lundeberg, T., 2003. Gender related differences in pain in spinal cord injured individuals. Spinal Cord 41 (2), 122–128.
North, R.Y., Li, Y., Ray, P., Rhines, L.D., Tatsui, C.E., Rao, G., Johansson, C.A., Zhang, H., Kim, Y.H., Zhang, B.o., Dussor, G., Kim, T.H., Price, T.J., Dougherty, P.M., 2019. Electrophysiological and transcriptomic correlates of neuropathic pain in human dorsal root ganglion neurons. Brain 142 (5), 1215–1226.
Obreja, O., Rathee, P.K., Lips, K.S., Distler, C., Kress, M., 2002. IL-1 beta potentiates heat-activated currents in rat sensory neurons: involvement of IL-1RI, tyrosine kinase, and protein kinase C. FASEB J. 16 (12), 1497–1503.
Odem, M.A., Bavencoffe, A.G., Cassidy, R.M., Lopez, E.R., Tian, J., Dessauer, C.W., Walters, E.T., 2018. Isolated nociceptors reveal multiple specializations for generating irregular ongoing activity associated with ongoing pain. Pain 159 (11), 2347–2362.
Odem, M.A., Lacagnina, M.J., Katzen, S.L., Li, J., Spence, E.A., Grace, P.M., Walters, E.T., 2019. Sham surgeries for central and peripheral neural injuries persistently enhance pain-avoidance behavior as revealed by an operant conflict test. Pain 160 (11), 2440–2455.
Pitcher, G.M., Henry, J.L., 2000. Cellular mechanisms of hyperalgesia and spontaneous pain in a spinalized rat model of peripheral neuropathy: changes in myelinated afferent inputs implicated. Eur. J. Neurosci. 12 (6), 2006–2020.
Price, T.J., Basbaum, A.I., Bresnahan, J., Chambers, J.F., De Koninck, Y., Edwards, R.R., Ji, R.R., Katz, J., Kavelaars, A., Levine, J.D., Porter, L., Schechter, N., Sluka, K.A., Terman, G.W., Wager, T.D., Yaksh, T.L., Dworkin, R.H., 2018. Transition to chronic pain: opportunities for novel therapeutics. Nat. Rev. Neurosci. 19 (7), 383–384.
Queiroz, B.F.G., Almeida, M.P.A., Bakhle, Y.S., Francischi, J.N., 2018. Calcitonin-gene related peptide is a potent inducer of oedema in rat orofacial tissue. Neuropeptides 68, 43–48.
Rau, K.K., McIlwrath, S.L., Wang, H., Lawson, J.J., Jankowski, M.P., Zylka, M.J., Anderson, D.J., Koerber, H.R., 2009. Mrgprd enhances excitability in specific populations of cutaneous murine polymodal nociceptors. J. Neurosci. Offi. J. Soc. Neurosci. 29 (26), 8612–8619.
Ray, P.R., Khan, J., Wangzhou, A., Tavares-Ferreira, D., Akopian, A.N., Dussor, G., Price, T.J., 2019. Transcriptome analysis of the human tibial nerve identifies sexually dimorphic expression of genes involved in pain, inflammation, and neuro-immunity. Front. Mol. Neurosci. 12, 37.
Rekand, T., Hagen, E.M., Gronning, M., 2012. Chronic pain following spinal cord injury. Tidsskr. Nor. Laegeforen. 132 (8), 974–979.
Richards, J.S., 2005. Spinal cord injury pain: impact, classification, treatment trends, and implications from translational research. Rehabil. Psychol. 50 (2), 99–102.
Rowe, P.S., Matsumoto, N., Jo, O.D., Shih, R.N., Oconnor, J., Roudier, M.P., Bain, S., Liu, S., Harrison, J., Yanagawa, N., 2006. Correction of the mineralization defect in hyp mice treated with protease inhibitors CA074 and pepstatin. Bone 39 (4), 773–786.
Rowe, P.S., Zelenchuk, L.V., Laurence, J.S., Lee, P., Brooks, W.M., McCarthy, E.T., 2015. Do ASARM peptides play a role in Nephrogenic Systemic Fibrosis? Am. J. Physiol. Renal Physiol. 309 (9), F764–F769.
Roza, C., Reeh, P.W., 2001. Substance P, calcitonin gene related peptide and PGE2 co-released from the mouse colon: a new model to study nociceptive and inflammatory responses in viscera, in vitro. Pain 93 (3), 213–219.
Saito, S., Mori, Y., Yoshioka, Y., Murase, K., 2012. High-resolution ex vivo imaging in mouse spinal cord using micro-CT with 11.7T-MRI and myelin staining validation. Neurosci. Res. 73 (4), 337–340.
Sandkuhler, J., 2006. Long-term potentiation and long-term depression in the spinal cord. In: Schmidt, R.F., Willis, W.D. (Eds.), Encyclopedia of Pain. Springer-Verlag, Berlin.
Sandkuhler, J., 2007. Understanding LTP in pain pathways. Molecular pain 3, 9.
Sandkuhler, J., Liu, X., 1998. Induction of long-term potentiation at spinal synapses by noxious stimulation or nerve injury. Eur. J. Neurosci. 10 (7), 2476–2480.
Siddall, P.J., Loeser, J.D., 2001. Pain following spinal cord injury. Spinal Cord 39 (2), 63–73.
Siddall, P.J., McClelland, J.M., Rutkowski, S.B., Cousins, M.J., 2003. A longitudinal study of the prevalence and characteristics of pain in the first 5 years following spinal cord injury. Pain 103 (3), 249–257.
Siney, L., Brain, S.D., 1996. Involvement of sensory neuropeptides in the development of plasma extravasation in rat dorsal skin following thermal injury. Br. J. Pharmacol. 117 (6), 1065–1070.
Sivilotti, L.G., Thompson, S.W., Woolf, C.J., 1993. Rate of rise of the cumulative depolarization evoked by repetitive stimulation of small-caliber afferents is a predictor of action potential windup in rat spinal neurons in vitro. J. Neurophysiol. 69 (5), 1621–1631.
Smith, G.D., Gunthorpe, M.J., Kelsell, R.E., Hayes, P.D., Reilly, P., Facer, P., Wright, J.E., Jerman, J.C., Walhin, J.P., Ooi, L., Egerton, J., Charles, K.J., Smart, D., Randall, A.D., Anand, P., Davis, J.B., 2002. TRPV3 is a temperature-sensitive vanilloid receptor-like protein. Nature 418 (6894), 186–190.
Soler, M.D., Kumru, H., Vidal, J., Pelayo, R., Tormos, J.M., Fregni, F., Navarro, X., Pascual-Leone, A., 2010. Referred sensations and neuropathic pain following spinal cord injury. Pain 150 (1), 192–198.
Sorge, R.E., LaCroix-Fralish, M.L., Tuttle, A.H., Sotocinal, S.G., Austin, J.S., Ritchie, J., Chanda, M.L., Graham, A.C., Topham, L., Beggs, S., Salter, M.W., Mogil, J.S., 2011. Spinal cord Toll-like receptor 4 mediates inflammatory and neuropathic hypersensitivity in male but not female mice. J. Neurosci. 31 (43), 15450–15454.
Staines, K.A., Mackenzie, N.C., Clarkin, C.E., Zelenchuk, L., Rowe, P.S., MacRae, V.E., Farquharson, C., 2012. MEPE is a novel regulator of growth plate cartilage mineralization. Bone 51 (3), 418–430.
Sullivan, P.G., Krishnamurthy, S., Patel, S.P., Pandya, J.D., Rabchevsky, A.G., 2007. Temporal characterization of mitochondrial bioenergetics after spinal cord injury. J. Neurotrauma 24 (6), 991–999.
Sun, R.Q., Tu, Y.J., Lawand, N.B., Yan, J.Y., Lin, Q., Willis, W.D., 2004. Calcitonin gene-related peptide receptor activation produces PKA- and PKC-dependent mechanical hyperalgesia and central sensitization. J. Neurophysiol. 92 (5), 2859–2866.
Tal, M., 1999. A role for inflammation in chronic pain. Curr. Rev. Pain 3 (6), 440–446.
Treede, R.D., Meyer, R.A., Raja, S.N., Campbell, J.N., 1992. Peripheral and central mechanisms of cutaneous hyperalgesia. Prog. Neurobiol. 38 (4), 397–421.
Vriens, J., Owsianik, G., Hofmann, T., Philipp, S.E., Stab, J., Chen, X., Benoit, M., Xue, F., Janssens, A., Kerselaers, S., Oberwinkler, J., Vennekens, R., Gudermann, T., Nilius, B., Voets, T., 2011. TRPM3 is a nociceptor channel involved in the detection of noxious heat. Neuron 70 (3), 482–494.
Wall, P.D., Devor, M., 1983. Sensory afferent impulses originate from dorsal root ganglia as well as from the periphery in normal and nerve injured rats. Pain 17 (4), 321–339.
Wall, P.D., Woolf, C.J., 1984. Muscle but not cutaneous C-afferent input produces prolonged increases in the excitability of the flexion reflex in the rat. J. Physiol. 356, 443–458.
Wall, P.D., Woolf, C.J., 1986. The brief and the prolonged facilitatory effects of unmyelinated afferent input on the rat spinal cord are independently influenced by peripheral nerve section. Neuroscience 17 (4), 1199–1205.
Walters, E.T., 2012. Nociceptors as chronic drivers of pain and hyperreflexia after spinal cord injury: an adaptive-maladaptive hyperfunctional state hypothesis. Front. Physiol. 3, 309.
Werhagen, L., Hultling, C., Molander, C., 2007. The prevalence of neuropathic pain after non-traumatic spinal cord lesion. Spinal Cord 45 (9), 609–615.
Woller, S.A., Hook, M.A., 2013. Opioid administration following spinal cord injury: implications for pain and locomotor recovery. Exp. Neurol. 247, 328–341.
Woodbury, C.J., Ritter, A.M., Koerber, H.R., 2001. Central anatomy of individual rapidly adapting low-threshold mechanoreceptors innervating the "hairy" skin of newborn mice: early maturation of hair follicle afferents. J. Comp. Neurol. 436 (3), 304–323.
Woolf, C.J., 1996. Windup and central sensitization are not equivalent. Pain 66 (2–3), 105–108.
Woolf, C.J., McMahon, S.B., 1985. Injury-induced plasticity of the flexor reflex in chronic decerebrate rats. Neuroscience 16 (2), 395–404.

Xu, X.J., Dalsgaard, C.J., Wiesenfeld-Hallin, Z., 1992. Spinal substance P and N-methyl-D-aspartate receptors are coactivated in the induction of central sensitization of the nociceptive flexor reflex. Neuroscience 51 (3), 641–648.

Xu, H., Ramsey, I.S., Kotecha, S.A., Moran, M.M., Chong, J.A., Lawson, D., Ge, P., Lilly, J., Silos-Santiago, I., Xie, Y., DiStefano, P.S., Curtis, R., Clapham, D.E., 2002. TRPV3 is a calcium-permeable temperature-sensitive cation channel. Nature 418 (6894), 181–186.

Xu, X.J., Zhang, X., Hokfelt, T., Wiesenfeld-Hallin, Z., 1995. Plasticity in spinal nociception after peripheral nerve section: reduced effectiveness of the NMDA receptor antagonist MK-801 in blocking wind-up and central sensitization of the flexor reflex. Brain Res. 670 (2), 342–346.

Yang, Q., Wu, Z., Hadden, J.K., Odem, M.A., Zuo, Y., Crook, R.J., Frost, J.A., Walters, E. T., 2014. Persistent pain after spinal cord injury is maintained by primary afferent activity. J. Neurosci. 34 (32), 10765–10769.

Zambrano-Rodriguez, P.C., Bolanos-Puchet, S., Reyes-Alva, H.J., de Los Santos, R.A., Martinez-Cruz, A., Guizar-Sahagun, G., Medina, L.A., 2021. High-resolution micro-CT myelography to assess spinal subarachnoid space changes after spinal cord injury in rats. J. Neuroimag. 31 (1), 79–89.

Zelenchuk, L.V., Hedge, A.-M., Rowe, P.S.N., Heymann, D., 2014. PHEX mimetic (SPR4-Peptide) corrects and improves HYP and wild type mice energy-metabolism. PLoS ONE 9 (5), e97326.

Zelenchuk, L.V., Hedge, A.M., Rowe, P.S., 2015. Age dependent regulation of bone-mass and renal function by the MEPE ASARM-motif. Bone 79, 131–142.

Zelenchuk, L., Hedge, A., Rowe, P.S., 2015. SPR4-peptide alters bone metabolism of normal and HYP mice. Bone 72, 23–33.